

Experimental verification of field-circuit model of a single-phase capacitor induction motor

Abstract. These The paper presents experimental verification of the 2D field-circuit model of the single-phase capacitor induction motor. Developed the field-circuit model was implemented for simulation using Flux2D software package. The verification of the 2D field-circuit model was conducted for starting of the motor with no-load, steady-state performance and at no-load and locked-rotor tests. Computed dynamic and steady-state characteristics were compared with measured ones to confirm correctness of the simulation model. The model is useful for study the effect of parameters of the motor on starting and running performance at desired load.

Streszczenie. Artykuł przedstawia weryfikację eksperymentalną dwuwymiarowego modelu polowo-obwodowego jednofazowego silnika indukcyjnego z pomocniczym uzwojeniem kondensatorowym. Opracowany model obliczeniowy zaimplementowano w środowisku Flux2D. Weryfikację przeprowadzono dla rozruchu silnika bez obciążenia, stanu ustalonego pracy. W celu oceny poprawności modelu porównano charakterystyki obliczone z pomierzonymi. Model może być przydatny do badań wpływu parametrów na właściwości rozruchowe oraz pracę znamionową badanego silnika. (Weryfikacja eksperymentalna dwuwymiarowego modelu polowo-obwodowego jednofazowego silnika indukcyjnego z pomocniczym uzwojeniem kondensatorowym).

Keywords: fractional horse power, single-phase, induction motor, field-circuit model, verification

Słowa kluczowe: moc ułamkowa, jednofazowy, silnik indukcyjny, polowo-obwodowy model, weryfikacja

Introduction

Single-phase capacitor induction motors are widely used as an electric drive for various appliances such as fans, blowers, pumps and compressors. The main and auxiliary stator windings have usually different number of turns, wire size and turns distribution along the periphery of the stator. This is the reason that mmfs produced by the stator winding currents is generally unbalanced. By using the capacitor connected in series with the auxiliary stator winding, the auxiliary winding current leads the main winding current by somewhat less than 90 electrical degrees. The auxiliary winding and the capacitor should be designed for better operation of the motor (e.g. at higher efficiency, power factor and lower torque pulsations) at any desired load (a specific operating point) [3-5]. To obtain high starting torque, the starting capacitor of appropriate value should be used, which is cut out after starting of the motor. For analysis performance of the capacitor induction motor the two-dimensional field-circuit model of induction motor has been implemented. The 2D field-circuit model does not allow for skew effect modeling but enables taking into account non-linearity of magnetic core and induced eddy currents in the rotor bars. In the paper, the field-circuit model of the single-phase capacitor induction motor is described and simulation results (using Flux2D [6]) of some dynamic and steady-state performance of the tested motor together with experimental ones have been presented.

Field-circuit model of capacitor induction motor

A coupled electric circuit is shown in Fig.1, in which L_m and L_a are end-winding inductances of stator winding, C_1 is run capacitor, V_1 is voltage source and Q_1 represents squirrel cage rotor and Z_1 is ground. The main (BM) and auxiliary (BA) windings are incorporated into to the finite element software and take into account the winding resistances.

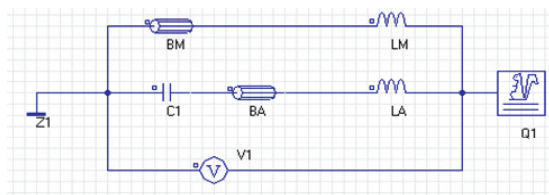


Fig 1 Coupled electric circuit of finite element analysis

An inductance of end-winding of stator and resistance and inductance of segment of end-ring of rotor are considered as constants. On basis of geometrical, material and winding data field-circuit model of analysed single-phase capacitor induction motor was implemented in Flux2D package (Fig. 2). The model takes into account nonlinear material of laminated core, eddy current induced in rotor bars and nonlinearities of magnetic core.

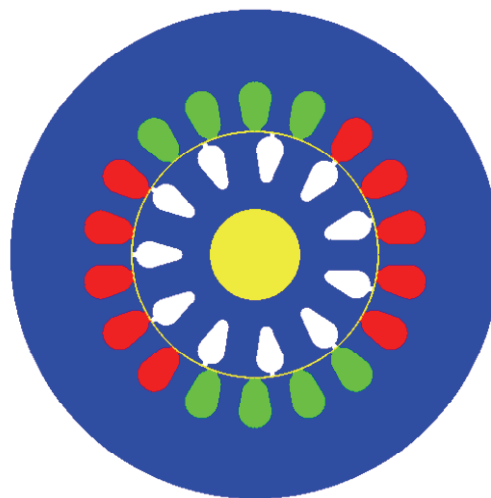


Fig 2 Two-dimensional field-circuit model of single-phase motor

In the stator there are two windings: the main (red) and auxiliary (green) which are distributed in 18 slots. Laminated core material is the M600-50A steel sheet (blue). The squirrel cage rotor consists of 11 aluminum bars (white). The mechanical shaft (yellow) is made of ST3 steel. The airgap is border of rotor set movement. The stator mechanical set is fixed. The model is discretised by a finite element mesh of 31000 nodes. All simulations was performed by transient magnetic application of Flux2D. Computed magnetic flux distribution for nominal speed of the motor (2840 rev/min) is shown in Fig. 3.

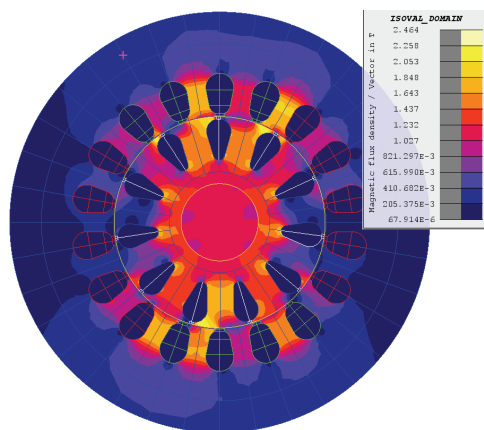


Fig 3 Magnetic flux distribution at nominal speed

Numerical simulation and measuring verification of the model

Experimental verification of the 2D FE field-circuit model of the single-phase capacitor induction motor was conducted for the following states of operation:

- starting of the motor at no-load until steady-state is reached,
- no-load test at constant speed,
- steady-state performance by varying load,
- locked-rotor test at voltage frequency of 50Hz.

Configuration of a measurement setup used for testing of the motor is shown in Fig. 4.

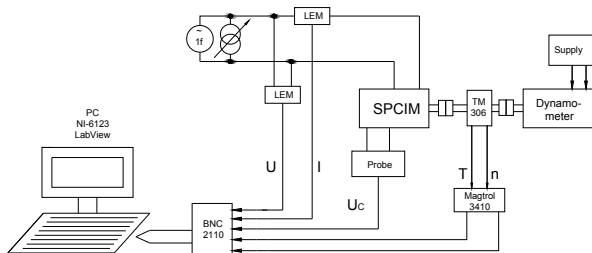


Fig.4. Measurement setup of single-phase capacitor induction motor

The setup allows measuring the following electrical and mechanical quantities of the motor:

- voltage and intake current
- rotational speed and output torque
- voltage across capacitor

Using the LabView virtual instrument all data for transient electrical and mechanical waveforms may be recorded and then processed by algorithm developed in the Matlab software.

All simulations was performed by transient magnetic application of Flux2D. The static trials were performed by transient magnetic application with imposed speed: 0 for locked rotor and 2980 rev/min for no-load. In case of steady state the speed was changing in range of 0-3000 with step of 200 rpm. In case of the free acceleration the coupled load option was used. Time step of simulation and acquisition was 1 ms.

The locked-rotor test of the motor was performed at rated frequency of 50Hz and voltage ranging from zero up to rated value which is possible for small power electric motors of low value of locked-rotor current. Since the motor torque depends on position of the rotor with respect to the stator, a preliminary test was carried out to determine the angular position of the rotor at which the minimum torque is developed. Measured and calculated quantities for nominal voltage are listed in Table 1.

Table 1 Computed and measured locked-rotor data of tested motor for locked-rotor

	I [A]	T [N·m]	P [W]	cosφ [-]
Test	2,01	0,17	420,5	0,89
Flux2D	2,01	0,17	416	0,86

The no-load test was conducted at rated frequency and constant speed of the running motor for voltages ranging from 120% of rated voltage down to a point where the current increases. The simulation was performed analogous by varying the amplitude of voltage source for speed n=2980 rpm. Measured and calculated quantities for no-load test at rated voltage are listed in Table 2

Table 2 Computed and measured data for no-load operation of tested motor

	I [A]	P [W]	cosφ [-]
Test	0,74	85,8	0,51
Flux2D	0,73	83,5	0,49

Steady-state operation of tested motor was carried out varying the load by means of dynamometer. Because the torque produced by used dynamometer was very low for low speed, only the stable part of the mechanical characteristic was tested. The measured and calculated results at nominal load are listed in Table 3.

Table 3 Computed and measured data for rated power operation

	I[A]	T[N·m]	P _r [W]	η [-]	cosφ [-]
Test	0,82	0.30	156,3	0,57	0,83
Flux2D	0,77	0.31	151,6	0,58	0,84

The measured and calculated data for above operation states show satisfactory agreement of convergence. More detailed results of steady state operation of tested capacitor motor can be found in paper [1,2]. Simulated and measured waveforms of starting of the motor with no-load are presented in Fig. 5. Computed intake current, output torque, speed and voltage across the running capacitor of tested motor are shown in Figs. 5a-d and the experimental ones are presented in Fig. 5e-5h for comparison.

The simulated waveforms at no-load starting of the motor showed satisfactory degree of convergence with the ones obtained by measurements. Some discrepancies may be observed in the output torque waveforms due to neglecting iron losses in the simulated model and unavoidable vibration of the actual motor under testing. It should be mentioned that the moment of starting is hard to simulate due to discrepancy in phase between calculated and measured current.

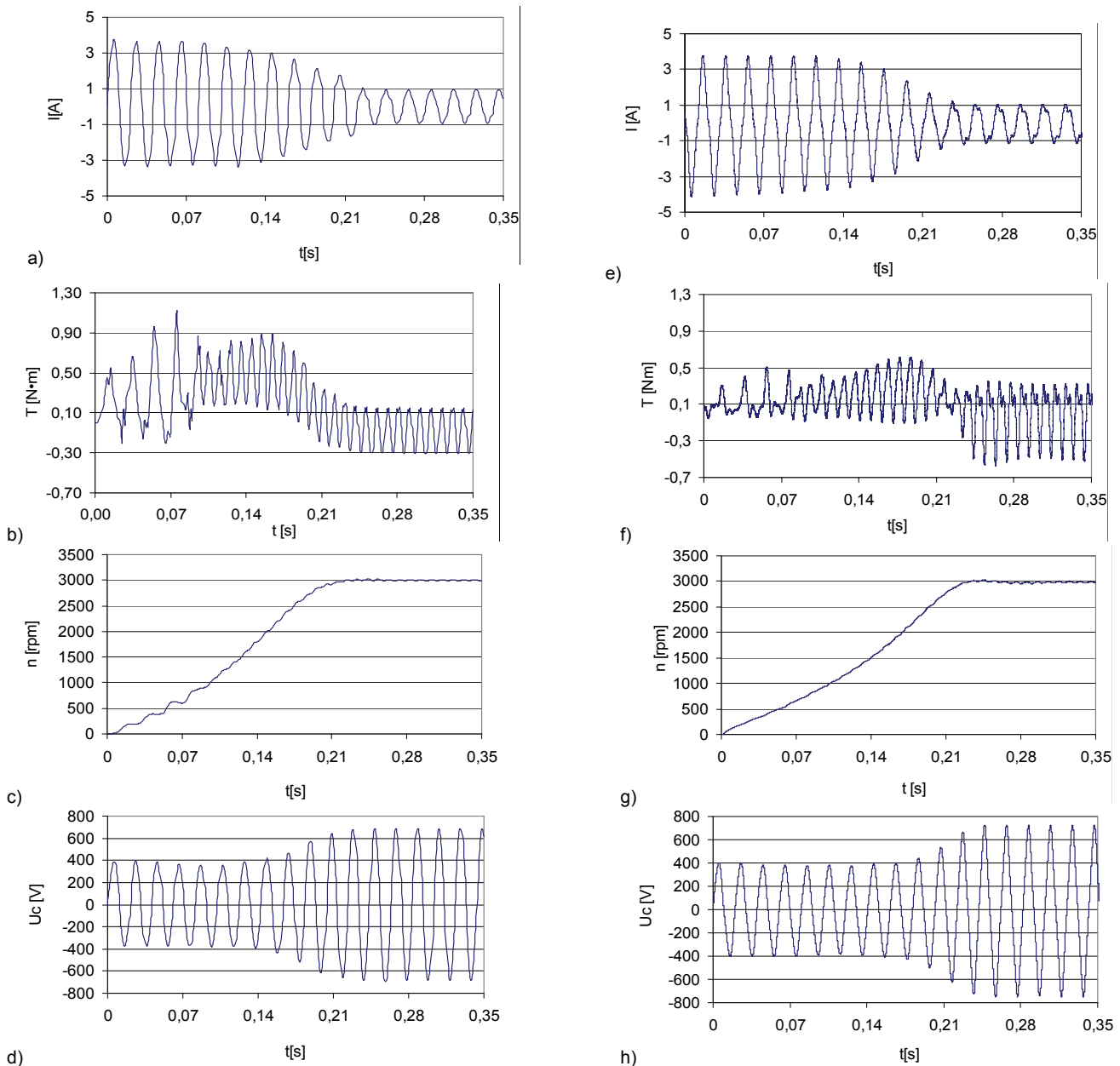


Fig. 5 Simulated (a,b,c,d) and measured (e,f,g,h) waveforms of intake current, output torque, rotational speed and voltage across capacitor of tested motor at no-load starting

Conclusion

The implemented 2D field-circuit model of the single-phase capacitor induction motor was experimentally verified from point of view its usefulness for simulation and study of performance characteristics of the single-phase capacitor induction motor at dynamic and steady state operation. The values of output parameters achieved for no-load, load and locked-rotor operation were compared with measured ones and confirmed correctness of the simulation model. Some discrepancies which occurred between simulation and measuring results in torque and current are caused by inaccuracy in modelling of magnetization characteristic of the magnetic core of the motor and by non-sinusoidal shape of the supply voltage in laboratory during conducting the tests (4% of THD).

REFERENCES

- [1] K. Makowski, M.J. Wilk, Field-circuit simulation of operation characteristics of the single-phase capacitor induction motor, *Electrical Review*, R. 86 NR 4/2010, pp. 213-216 (in Polish)
- [2] K. Makowski, M.J. Wilk, Steady-state investigation of single-phase capacitor induction motor, *Electrical Review*, R. 88, NR 2/2012, pp. 180-183,
- [3] W.H. Yeadon, A.W. Yeadon, Handbook of small electric motors, *McGraw-Hill*, 2001
- [4] G. Meunier, The Finite Element Method for Electromagnetic Modeling, *ISTE Publishing* 2008
- [5] Da Silva C.A., F. Bidaud, P. Herbert, Cardoso J.R., Power factor calculation by the finite element method, *IEEE Trans. Magn.*, Vol. 46, No. 8, 2010, pp 3002-3005
- [6] Flux2D v. 10.4, *User's guide*, CEDRAT, France

Authors: Krzysztof Makowski, D.Sc., Ph.D., Wrocław University of Technology, Institute of Electrical Machines, Drives and Measurements, Poland,
e-mail: krzysztof.makowski@pwr.wroc.pl
Ph.D. student Marcin J. Wilk, M.Sc., Wrocław University of Technology, Institute of Electrical Machines, Drives and Measurements, Poland,
e-mail: marcin.j.wilk@pwr.wroc.pl